Dear Editors and Referees,

We owe our great thanks to the editor and the referees for the evaluation of our article. The criticisms and suggestions have been helping us think over some questions in our investigation and improve our manuscript much.

According to the suggestions and comments of the referees, the manuscript has been revised:

1. The abstract and summary were rewritten so that it is in consistence with the text and conclusions, according to the suggestions of the referees.

2. Figure 1 was regenerated to remove the redundant plots according to one referee's suggestion, only the X-Y and Y-Z plots were remained.

3. Based on more accurate estimate of the magnetosheath velocity, the low-density and high velocity feature was confirmed, the V_m-N_i plot in figure 5 was regenerated with more data points in the low-density and high velocity region. Some further discussions were also added to the text correspondingly.

4. The results of the MVA were discussed more in the text, and a table of the results was added to the manuscript, to show the reliability of MVA in this event.

5. Per one referee's comments, further discussion was added to the text on the plasma transport, some descriptions were deleted to avoid confusing or misunderstanding.

6. Figure 3 was revised. The illustrations of V_m, V_n, ΔB_m, ΔB_n were added to the scales on the right side of panels 3-6 to make the plots easier to read.

7. Some references were added to the reference list.

8. Some other mistakes were corrected in the text.

9. The Data availability, Author contribution and Competing interest were added to the manuscript as required by the system.

Reply to Anonymous Referee #1

Thank you very much for spending time to evaluate our article. Your comments and criticisms will help us to improve our understanding of the observations in this event and to find more accurate descriptions. Based on our thinking over some questions involved in this event, we would like to respond as follows: Your original comments and questions are in blue and our responses are in black.

The paper reports observations of Kelvin-Helmholtz (KH) vortices by two THEMIS spacecraft (THA and THE) at the dusk magnetopause, dayside of the terminator. The periodic crossings of the magnetopause occurred following a northward turning of the interplanetary magnetic field. The identification of the vortices is based on the computation of boundary normal directions via minimum variance analysis (MVA). Interestingly, low density plasma faster than magnetosheath plasma – a common feature of KH vortices – was not observed. The spacecraft locations allow for an assessment of C1 the evolution of the vortices: Crossing of regions with mixed magnetospheric and magnetosheath plasmas appear more/less periodic at an earlier/later stage, suggesting the transport of plasma across the magnetopause.

My main criticism is related to the identification of vortices and the interpretation of observations supporting the hypothesis of plasma transport across the magnetopause. At this point, I do not think that the conclusions of the paper are sufficiently supported by the observations.

Specific comments:

1) It is not convincingly shown that the magnetopause oscillations observed are actually due to the passage of magnetopause KH vortices and not, e.g., due to the passage of magnetopause surface waves that have not yet reached the non-linear stage. In this study, vortices are mainly identified by a sequence of boundary normal vectors, obtained from MVA applied to magnetic field observations (e.g., line 122+). However, MVA results can strongly depend on the selected time intervals around current sheets to which the method is applied. It would help enormously if the authors could assess the stability and reliability of the MVA results, also taking into account the eigenvalue ratios as described by Sergeev et al. (Ann. Geophys., 2006). I am doubtful about the reliability of MVA results here, because the magnetic field variations that can be analyzed are not particularly strong (see panels 3 and 7 of Figure 2).

We think it right that the MVA results strongly depend on the selected time intervals that cover the magnetopause. In this event, the IMF is strongly northward, and the observed magnetic field doesn't change much, so it could be difficult to identify the magnetopause. So, we selected the four intervals when the TH-A ion spectrum shows the magnetosheath feature (absence of the magnetospheric hot ions) to calculate the local boundary coordinates. We operated the MVA method carefully by using the high resolution magnetic field data, and by identifying the magnetopause in the ion spectrum. In diagnosing the MVA results, we also selected the better results with relative larger ratios between the eigenvalues. As you suggested above, we would like to show the details of the MVA analysis in a table, which will also be added to the revision of our article. In the MVA results, it can be seen that 4 of 8 eigenvalue ratios are larger than 3, indicating the reliability of the MVA method at their corresponding crossings, even though the magnetic field doesn't change strongly. At least at these traversals, the magnetopause was deformed to the nonlinear vortices.

Table 1. results of MVA analysis at the four magnetosheath encounters.

Num	Time interval	L	M	N	$r_{23} = \varepsilon_2/\varepsilon_3$
1	22:23:50-22:24:12	0.0637 -0.3955 0.9162	0.4374 -0.8141 -0.3819	0.8970 0.4251 0.1212	4.56
2	22:24:20-22:25:15	0.0646 -0.2602 0.9634	-0.3877 0.8830 0.2645	-0.9195 -0.3906 -0.0438	5.27
3	22:32:30-22:32:52	0.0017 -0.6860 0.7276	0.8349 -0.3995 -0.3786	0.5504 0.6081 0.5721	1.82
4	22:32:52-22:33:14	-0.0561 0.3303 0.9422	-0.3946 0.8595 -0.3248	-0.9171 -0.3900 0.0821	2.25
5	22:35:35-22:36:00	0.2636 -0.4912 0.8302	0.1004 -0.8420 -0.5301	0.9594 0.2231 -0.1726	3.34
6	22:36:07-22:36:20	-0.0102 0.0117 0.9999	0.3363 0.9417 -0.0076	-0.9417 0.3362 -0.0135	2.77
7	22:38:41-22:39:05	0.2307 -0.4125 0.8813	0.0363 -0.9014 -0.4314	0.9724 0.1315 -0.1930	3.42
8	22:39:05-22:40:30	-0.0574 -0.7802 0.6229	-0.5073 -0.5145 -0.6913	-0.8599 0.3556 0.3662	1.07

Furthermore, I am concerned about the identification of KH vortices in the absence of low density plasma that is faster than the magnetosheath plasma (e.g., line 141+). This feature has been used to identify vortices using single spacecraft measurements. It may also be observed without vortices being present: the passage of a surface wave should suffice. But if vortices are present, then the feature should be observable too, and I cannot find any statement in Masson and Nykyri (2016) that would suggest the opposite. So the absence of that feature indicates, in my opinion, that the oscillations are rather related to a magnetopause surface wave rather than to KH vortices. Note that rotations in the bulk velocity, magnetic field deviations, and distortions of the magnetopause can also result from magnetopause surface waves (e.g., line 205).

We agree that the high-speed low-density feature is one of the typical characteristics of the K-H vortices and very useful in diagnosing the K-H vortices in single spacecraft measurements. It was a surprise to us that the high-speed low-density feature did not appear in the Ni-Vm plot in this event. We used to estimate the magnetosheath velocity by drawing a horizontal line that is close to most of the magnetosheath intervals shown in panel 4 of figure 2. The horizontal line was at the velocity of about 180 km/s. Now, we re-estimate the magnetosheath velocity by averaging the TH-A measurements during the four magnetosheath intervals, with the more accurate velocity of about 134 km/s in the magnetosheath. Based on the new estimation, the high-speed low-density feature can be seen in the Ni-Vm plot, with more data points distributed in blue box (see the revised figure 5 below). The high-speed low-density feature can support the K-H vortices in this event.

Furthermore, the linear surface waves could not explain the fine structure of the observed first perturbation in TH-E observations, shown in the additional figure below, which is worthy of an independent article and we are further working on, with new results of the micro-physical process to transport solar wind into magnetosphere within the K-H vortices. The double peaks in the ion measurements can be caused either by second traversal of the non-linear K-H vortex or by the secondary substructure of the vortex. More details of the plasma transport in the K-H vortex will be revealed in another article in preparation.

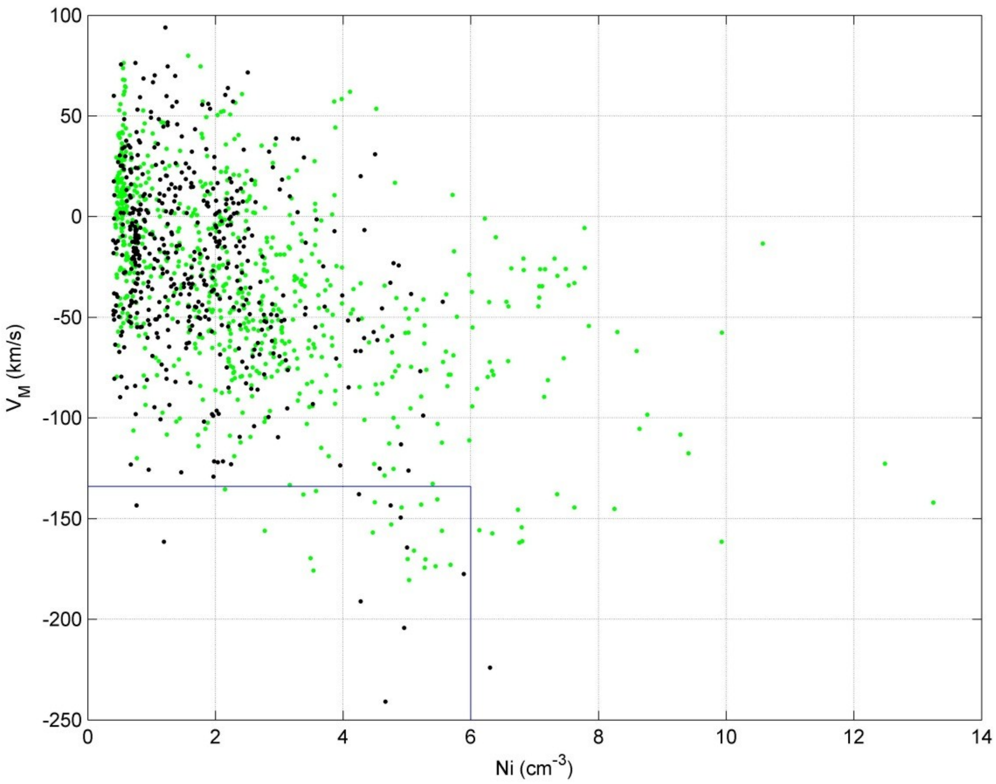

Figure 5. The observed velocity along the tailward direction versus the ion density. Green dots are from TH-A observations and black dots from TH-E observations. The blue lines mark the high-speed and low density region possibly caused by the acceleration of the rotation.

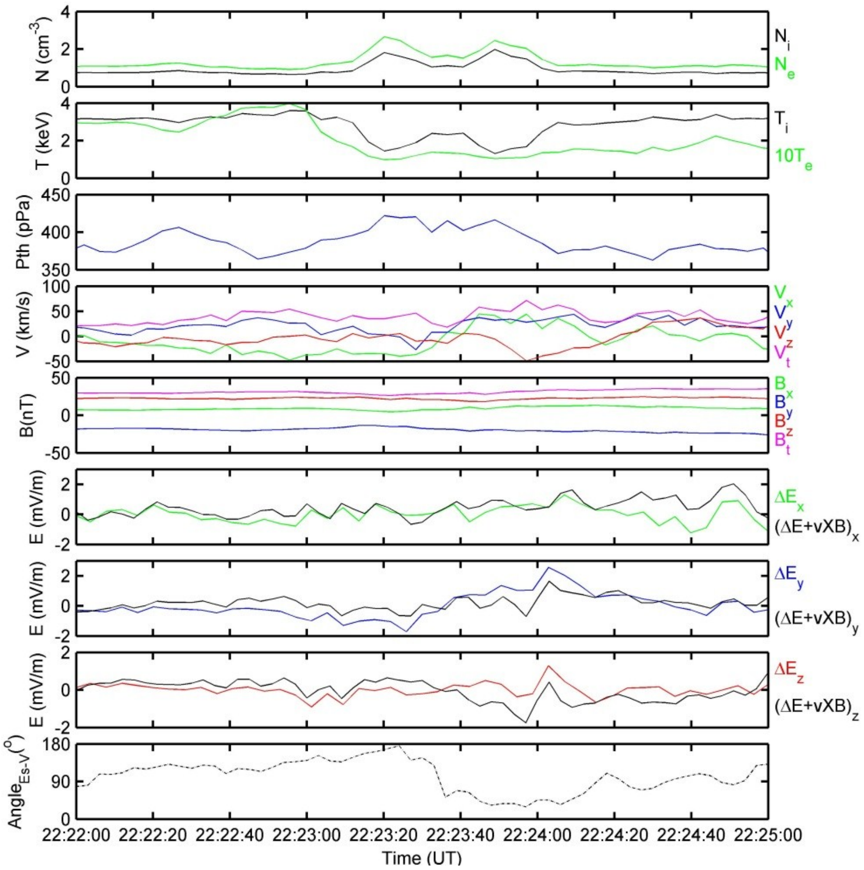

Additional figure, which is not enclosed in this article, to show the double peaks in TH-E plasma observations. The linear surface waves could not explain the double peaks. The new results of the micro-physical process to transport solar wind into magnetosphere within the K-H vortices are worthy of another independent article.

2) It is not convincingly shown that a significant and unambiguous plasma transport took place across the magnetopause (e.g., lines 211, 214). This main conclusion of the paper is inferred from observation of less periodic features seen by THE in comparison to THA, the former being located further down the tail from the latter. I would at least expect some further discussion on how this strong conclusion can be drawn from the observations (e.g., by putting the results into the context of prior observations or simulations). However, also the observations themselves are not consistent over the presented time interval: As can be seen in Figure 2, THA sees more periodic magnetopause oscillations before 22:40 UT, as discussed in the paper. After 22:40, THE sees very periodic oscillations and THA observations are “more dispersed” (e.g., between 22:44 and 22:51). Following the argument in the manuscript, plasmas should have unmixed while vortices moved from THA to THE during this period of time.

Thank you for your comments that can further help our thinking over some questions in this event. Above all, word “unambiguous” in conclusion has been deleted so that it is not so strong. The coexistence of hot and cold ions is one of direct feature of the solar wind transport into magnetosphere, as clearly displayed in Geotail observations by Fujimoto et. al. (1998) and in Cluster observations by Hasegawa et. al. (2004). In this event, the coexistence of hot and cold ions was firstly noted near the periodically oscillating magnetopause. Furthermore, we used the enhancement of hot electron flux as an indicator of the LLBL, and set up the more critical criteria to diagnose the coexistence, and hence to display the transport regions, as marked by the green bars at the bottom of panel 6 and black bars at the bottom of panel 10 in figure 2. Compared with the possible pre-existing LLBL before the perturbations, the coexistence of hot and cold ions shows the fresh entering of cold ions into the LLBL. The evidence of the plasma transport is clearly shown in this event. By comparing the green bars and the black bars, it can be found that the transport regions in TH-A observations appears more periodic but those in TH-E observations more dispersed. The difference between the features of transport regions at upstream TH-A and downstream TH-E implies the plasma transport significantly occurred and evolved during the tailward propagation, along with the collapse of the vortices, leading to a kind of turbulence state, as illustrated in previous simulations (Nakamura et al., 2004; Matsumoto & Hoshino, 2004).

You are right that TH-A observed very clearly periodic motions of magnetopause during the 34 minutes except UT 22:46-22:50 TH-E observed relatively much more dispersed spectrum during the interval but 5 clear periods of oscillations appeared again during UT 22:40-22:48. However, it seems true that on the whole the spectrum observed at TH-E is much more turbulent than the periodic spectrum at TH-A. Such characteristics imply the collapse of the vortices and the evolution leading to turbulence state. In previous simulations (Nakamura et al., 2004; Matsumoto & Hoshino, 2004), the vortices collapse and transport solar wind into magnetosphere, after that, new vortices may be generated at the recovered magnetopause. The 5 oscillations during UT 22:40-22:48 at downstream TH-E can by explained as newly formed vortices.

If you agree with the above discussion, it will be added to the text to enrich the understanding of observations in this event. Thank you for all your comments, criticisms and suggestions that help us to improve the article.

3) It is not convincingly shown that there was no pre-existing (low-latitude) boundary layer (LLBL), consisting of a mixture of magnetosheath and magnetospheric plasmas. This mixture is used as a synonym to plasma transport across the magnetopause in the paper (line 164), supposedly starting with the northward turning of the IMF. But a LLBL might have been present at the magnetopause even before the oscillations started. To confirm this or rule it out, we would need spacecraft observations across the magnetopause near the THEMIS positions before the event. However, such observations do not seem to be available, and both THA and THE were probably too far away from the magnetopause to observe a pre-existing LLBL. During the event, as the surface waves went by, the magnetopause moved periodically closer to the spacecraft so that they were able to enter the LLBL, as stated in line 204.

Thank you for your comments that have pushed us to think the question further. It is true that we need observations of another spacecraft nearby across the magnetopause to confirm or rule out the possible pre-existing denser layer. We tried using the MMS conjunction times but the four-spacecraft stellar were not located near THEMIS. From the observations in this event, we only know that neither of the 2 spacecraft of THEMIS near the magnetopause observed the pre-existing denser layer before the K-H waves (surface waves according to your comments). As you pointed out, “a LLBL might have been present at the magnetopause even before the oscillations started”. Unfortunately, we cannot confirm the absence of the pre-existing denser layer before the perturbations. So the description that “there is no pre-existing denser layer to facilitate the instability" has been deleted.

Thank you for your reminding us that the word "mixture" was inappropriately used as a synonym to plasma transport across the magnetopause. Mixture is a state of two components in plasma, such as the plasma in LLBL, while transport is a process of the transfer of solar wind into the magnetosphere. The LLBL is a result or consequence of the solar wind transport into magnetosphere. In this event, the most prominent characteristics are the periodic oscillations of the magnetopause, and the coexistence of hot and cold ions, with more emphasis on the transport process. So we are using the word "transport" and "coexistence" to describe the event. The "mixture region" in the caption of figure 6 was also replaced by "coexistence region" to avoid confusion.

4) I do not know what the authors exactly mean by "field-line stretching" (e.g., lines 22, 118) and how such a behavior would be reflected or identifiable in single spacecraft ion velocity or magnetic field time series.

Thank you for your suggestions. We used to describe the deformation of the magnetopause accompanied by the field line stretching as illustrated by Hasegawa et. al. (2004), the magnetic field was disturbed at the low latitude region. Actually, the magnetopause deformation can cause the magnetic deviations, and the deviations can be available in both linear surface waves and nonlinear vortices, as you mentioned in your comments. In order to avoid confusing or misunderstanding, the "field line stretching" has been deleted for more accurate description.

Minor comments on figures:

- Figure 1 conveys very little information. It may be sufficient to keep only the x-y-plot.

Thanks for your suggestion. We revised the figure by taking only the X-Y plot indicating the location near the magnetopause and the Y-Z plot indicating the low-latitude region.

- It may be helpful for the reader to state the meaning of the green and black bars in Figure 2 (below panels 6 and 10) in the caption.

Thank you for such a reminding. The description of the green and black bars has been added to the caption of figure 2.

- I cannot see any reason for the inverted time line in Figure 3. Please state a clear reason or display the data in the conventional way, with time moving forward to the right.

In this event, it was at the duskside of magnetopause, we displayed the vectors of the velocity and magnetic field perturbations not only in plots but also in arrowed lines (black lines in panels 3-6), with the scales of the magnitudes on the right side of each panel. The directions of M and N components correspond to the leftward and downward directions respectively, viewing from the Z direction. The data on the right side occur earlier than those on the left side, earlier data should be propagated more tailward to the rightside. We used the reverted time line (as Hasegawa et al. (2004) used in their publication in Nature) just in order to show the time sequence from right to left. The illustrations of V_m, V_n, ΔB_m, ΔB_n have been added to the scales on the right side of panels 3-6.

Reply to Anonymous Referee #2

Thank you very much for taking your valuable time to evaluate our article. Your endorsement, as well as your suggestions, is encouraging us to go further to investigate more details of the transport mechanism in K-H vortices. We have made minor modifications as you suggested, and would like to response as follows. Your original comments and questions are in blue and our responses are in black.

In this research, the authors have investigated the transport of the solar wind plasmas into the magnetosphere from the flank side during the northern IMF period, and present a clear evidence for the K-H instability mechanism. The THEMIS data are used and MVA method is applied to determine the configuration of the distorted magnetopause. The periodic K-H vortices are observed and there exists the mixture of the cold magnetosheath plasmas and hot magnetospheric plasmas within the vortices. This paper will enhance the understanding on the mechanism how the K-H instability drives the transport of the magnetosheath plasmas into the magnetotail plasma sheet. So it can be accepted for publication after minor modifications. Some comments on the paper are as the following.

(1) Line 127-129: L and M are tangential to the magnetopause, so the word “parallel” can be replaced by “tangential”. In line 129, the expression “the hangential and normal directions M-N” is proper.

Per your suggestion, the text has been revised. We have replaced “parallel” by “tangential”.

(2) Line 152-159: The values of the temperatures of the hot magnetospheric plasmas and cold magnetosheath ions and electrons can be given.

The typical temperatures are now given in the text.

(3) Line 347: The topic of the paper is not complete.

Sorry for the unexpected mistake. The topic of the paper has been complemented.

Plasma transport into the duskside magnetopause caused by Kelvin-Helmholtz vortices in response to the northward turning of the interplanetary magnetic field observed by THEMIS

Guang Qing Yan[1], George K. Parks[2], Chun Lin Cai[1], Tao. Chen[1], James P. McFadden[2], Yong Ren[1,3]

[1] State Key Laboratory of Space Weather, National Space Science Center, Chinese Academy of Sciences, Beijing, China, 100190

[2] Space Science Laboratory, University of California, Berkeley, California, USA, CA94720

[3] University of Chinese Academy of Sciences, Beijing, China, 100049

Abstract: A train of Kelvin-Helmholtz (K-H) vortices with plasma transport across the magnetopause has been observed by the Time History of Events and Macroscale Interactions during Substorms (THEMIS) at the duskside of magnetopause~~ when the interplanetary magnetic field (IMF) abruptly turns northward~~. This unique event ~~occurred ~~occurs when the interplanetary magnetic field (IMF) abruptly turns northward, which is the immediate change~~without pre-existing denser boundary layer ~~to facilitate the K-H instability. Two THEMIS spacecraft, TH-A and TH-E, separated by 3 Re, periodically encountered the duskside magnetopause and the low-latitude boundary layer (LLBL) with a period of 2 minutes and tailward propagation of ~~194 ~~212 km/s. T~~here was no high-velocity low-density feature, but t~~he rotations in the bulk velocity observation, distorted magnetopause with plasma parameter fluctuations and the magnetic field ~~line stretching~~perturbations, as well as high-velocity low-density feature, indicate the formation of rolled-up K-H vortices at the duskside of magnetopause. ~~A ~~The ~~mixture ~~coexistence of magnetosheath ions with magnetospheric ions and enhanced energy flux of hot electrons is identified in the K-H vortices. ~~This ~~These ~~mixture ~~transport regions appears more periodic at the upstream spacecraft and more dispersive at the downstream location, indicating a significant transport can occur and evolve during the tailward propagation of the K-H waves. There is still much work to fully understand the Kelvin-Helmholtz mechanism. The observations of direct response to the northward turning of the IMF, the ~~unambiguous ~~clear plasma transport within the vortices, involving both ion and electron fluxes can provide

additional clues to the K-H mechanism.

Key words: K-H vortices, northward IMF, plasma transport, LLBL

1 Introduction

Kelvin-Helmholtz (K-H) instability can be activated at the interface between different plasma regimes with different velocities, and the perturbations propagate along the direction of the velocity shear as a form of surface wave developing into nonlinear vortices. As shown by Hasegawa (1975), the high density and the magnetic field perpendicular to the velocity shear on either side of the interface facilitate the unstable condition. The fastest K-H instability occurs when the wave vector $\boldsymbol{k}$ is parallel/antiparallel to the velocity shear and perpendicular to the magnetic field (Southwood, 1979; Manuel & Samson, 1993). This condition favors the low-latitude magnetopause where the velocity shear and the northward magnetospheric magnetic field are available. The magnetic tension stabilizes the shear layer if the magnetic field and the velocity shear are aligned, indicating that the radial IMF does not favor the K-H instability. However, reported observation indicates that K-H waves occur at the high-latitude magnetopause under the dawnward IMF and continues to exist when the IMF turns radial (Hwang et al., 2012). On the other hand, under the radial IMF, K-H instability is found in both simulations (Tang et al., 2013; Adamson et al., 2016) and observations (Farrugia et al., 2014; Grygorov et al., 2016). In some cases, the K-H instability is thought facilitated by a denser boundary layer formed by the dayside magnetic reconnections (Grygorov et al., 2016), by the plasma plume (Walsh et al., 2015), or by the pre-existing denser boundary layer formed by the high-latitude reconnections under the northward IMF (Hasegawa et al., 2009; Nakamura et al. 2017). Theoretically, both northward and southward IMF can favor the K-H instability at the low-latitude magnetopause. In fact, almost all of the previous observations (Chen & Kivelson, 1993; Kivelson & Chen, 1995; Fujimoto et al., 2003; Hasegawa et al., 2004) and simulations (Chen et al., 1997; Farrugia et al., 2003; Miura, 1995; Hashimoto & Fujimoto, 2005) show that the K-H waves occur preferentially under the northward IMF, although linear K-H waves are observed under the southward IMF (Mozer et al., 1994; Kawano et al., 1994). However, under the southward IMF, Cluster has observed nonlinear K-H waves with irregular and turbulent characteristics (Hwang et al., 2011) and THEMIS has observed regular K-H vortices with an induced electric field at the edges (Yan et al., 2014). As reviewed (Johnson et al., 2014; Masson & Nykyri, 2016) recently, observations from many missions such as Cluster, THEMIS, Wind, Geotail etc., as well as simulations greatly enriched our understandings of the K-H instability and the vortices. ~~Recently~~Based on long term observations, a statistical survey indicates that K-H waves are much more ubiquitous than previously thought (Kavosi & Raeder, 2015), which implies the importance of the solar wind plasma transport into the magnetosphere via the K-H vortices.

In addition to magnetic reconnections at low latitude (Dungey, 1961) and high latitude magnetopause (Song & Russell, 1992), whose nature is a popular research topic (e.g., Dai, 2009; Dai et al., 2017; Dai, 2018), the K-H instability is an important way to transport solar wind into the magnetosphere when reconnections are inactive at the magnetopause. A statistical study of Double Star observations implies the entry of cold ions into the flank magnetopause caused by the K-H vortices that is enhanced by solar wind speed (Yan et al., 2005). However, it is noted that the

K-H instability itself cannot lead to plasma transport across the magnetopause (Hasegawa et al., 2004); therefore, certain secondary processes (e.g., Nakamura et al., 2004; Matsumoto & Hoshino, 2004; Chaston et al., 2007) are necessarily coupled with the K-H instability for plasma transport into the magnetosphere via the LLBL. The reconnection of the twisted magnetic field lines inside the K-H vortex was first found in a simulation (Otto & Fairfield, 2000) and has since been identified in observations (Nykyri et al., 2006; Hasegawa et al., 2009; Li, et al., 2016). The plasma transport into the magnetosphere via such a process in K-H vortices has been quantitatively investigated in a simulation (Nykyri & Otto, 2001). Most recently, energy transport from a K-H wave into a magnetosonic wave was estimated conserving energy in the cross-scale process, and three possible ways were discussed to transfer energy involving shell-like ion distributions, kinetic Alfvén waves, and magnetic reconnection (Moore et al., 2016). Up to now, reports of direct observations of plasma transport in the K-H vortices are only a hand full (e.g., Sckopke et al., 1981; Fujimoto et al., 1998; Hasegawa et al., 2004). Moreover, the microphysical processes for the plasma transport remains unclear, indicating more observations of such a transport process are needed to help us understand the physics. In this work, we present the THEMIS observations of the K-H vortices activated when the IMF abruptly turns northward, without a pre-existing denser boundary layer to facilitate the instability. We show a significant solar wind transport into the magnetosphere occurs and evolves within the vortices.

2 Data and Methods

The THEMIS mission (Angelopoulos, 2008) consists of five identical spacecraft originally orbiting the Earth similar to a string of pearls configuration. In August 2009, TH-B and TH-C were pushed to the vicinity of the lunar orbit, while the other three stayed in the near-Earth orbit with an apogee of approximately 13 Re. The instruments onboard include a flux gate magnetometer (FGM) (Auster et al., 2008) to measure the magnetic field and an electrostatic analyzer (ESA) (McFadden et al., 2008) to measure the electron (6 eV-30 keV) and ion (5 eV-25 keV) fluxes. We used the 3-second averaged FGM and ESA data from TH-A and TH-E to perform the particle analysis, and the 1/16 second averaged FGM data to perform the minimum variance analysis (MVA) (Sonnerup & Cahill, 1967; 1968) to determine the local magnetopause coordinates to find the distortions of the magnetopause. The FGM and ESA data from TH-B located in the dawnside downstream solar wind provide the IMF and solar wind conditions with an estimated time lag of 10 minutes from the subsolar magnetopause to TH-B. Both ion and electron energy spectra with a 3-second resolution were used to diagnose the ~~mixture~~ transport of the magnetosheath and magnetospheric ions. During the interval of interest, there are no data in the top energy channels centered at 25.21 keV for the ion spectrum and 31.76 keV for the electron spectrum, which has not influenced our investigations.

3 Observations and Discussions

During the interval UT 22:20-22:54 on March 28, 2016, TH-A and TH-E were located near the magnetopause (figure 1), while TH-D was located in the inner magnetosphere, far from the magnetopause. TH-B, near the lunar orbit, was immersed in the solar wind at the dawnside downstream of the other two spacecraft. As shown in panel 1 of figure 3, TH-B observed an abrupt turning of the IMF from duskward to northward at UT 22:32, corresponding to UT 22:22, with a time lag of 10 minutes ((10+32.7) Re / (450 km/s)) from the subsolar magnetopause to

TH-B. Periodical fluctuations were observed in both the TH-A and TH-E observations (figure 2), from ion density in panel 1, temperature in panel 2, magnetic field in panel 3 and 7, to velocity in panel 4 and 8, especially the alternating appearances of hot and cold ions in the energy-time spectra (panel 5 and 9). The period was approximately 2 minutes (17 peaks within 34 minutes), and the tailward bulk propagation speed was approximately 212~~195~~ km/s (3 Re / 90 s). In figure 3, the rotational characteristics were identified in the periodical fluctuations in V_l, V_m and V_n with phase differences between them. The magnetic field deviations in panels 3 and 5 indicated the ~~stretching~~ perturbations of the magnetic field along with the deformation of the magnetopause. The alternating appearances of the two different plasmas imply the multiple periodic encounters of the magnetopause and the LLBL, which is one of the typical characteristics of K-H vortices.

In this event, the IMF is strongly northward, and the observed magnetic field doesn't change much, so it could be difficult to identify the magnetopause. We selected the four intervals of UT 22:24:00-22:24:40, UT 22:32:40-22:33:10, UT 22:35:50-22:36:10, UT 22:28:50-22:39:20, marked by the black arrows, when the TH-A ion spectrum showed the magnetosheath feature~~At UT 22:24, UT 22:32, UT 22:36, UT 22:39,~~ . ~~marked by the black arrows,~~ During the four intervals, TH-A observed magnetosheath cold ions without magnetospheric hot ions (green regions at top of panel 5, figure 2). The absence of hot ions indicated that the spacecraft had crossed the magnetopause into the magnetosheath, where the outbound and inbound crossings of the magnetopause can be identified in the ion spectrum. At each pair of traversals, the local magnetopause coordinates LMN were calculated by using MVA (Sonnerup & Cahill, 1967; 1968). The details and results of MVA calculations are listed in table 1. In the calculations of MVA, relative large ratios of the second to third eigenvalues $r_{23} = \varepsilon_2/\varepsilon_3$ means better reliability of determination of local coordinates (e.g. Sergeev et. al., 2006). In the MVA results, it can be seen that 4 of 8 eigenvalue ratios are larger than 3, indicating the good reliability of the MVA method at their corresponding crossings, even though the magnetic field doesn't change strongly. At least at these traversals, the magnetopause was deformed to the nonlinear vortices. The calculated normal direction ***N*** as well as the ~~parallel~~ tangential direction ***M*** of the local magnetopause is used to identify the distorted magnetopause. In each panel of figure 4, the normal and ~~parallel~~ tangential directions ***M-N*** at the outbound and inbound magnetopause are plotted in the equatorial plane, compared with the average ***M-N*** of the magnetopause. The average magnetopause in dotted line, as well as the average ***M-N*** directions, is calculated from the model (Shue, 1998), and the dotted line is also approximately the trajectory of the spacecraft TH-A, which is moving at a relatively slow speed of about 2 km/s at the apogee. The distorted magnetopause is plotted in black line, perpendicular to ***N*** and parallel to ***M*** at outbound and inbound. The deviations of the ***M-N*** directions from the averaged magnetopause illustrate the magnetopause distortions formed by the K-H vortices. Such distortions of the magnetopause qualitatively explain the periodically alternating encounters of magnetosphere-like and magnetosheath-like plasmas. The plasma rotation is also illustrated by the red circle with arrow, consistent with the observations in panel 4 of figure 2.

带格式的：非上标/ 下标

The high-speed and low-density feature is one of the fundamental characteristics of rolled-up vortices (Nakamura et al., 2004; Takagi et al., 2006~~Hasegawa et al., 2006~~), ~~but not for every event (Masson & Nykyri, 2016), because the acceleration occurs only in certain stages of the development~~and has been used to identify vortices in a single spacecraft measurements (e.g., Hasegawa et al., 2006; Hwang et. al., 2011, Grygorov et al., 2016). We estimated the

带格式的：字体：(默认) Times New Roman

magnetosheath velocity by averaging the TH-A measurements during the four magnetosheath intervals mentioned above, with the magnetosheath velocity of about 134 km/s. Figure 5 shows the V_m-N_i plot, in which the blue lines mark the high-speed and low-density region. V_m is the tailward velocity, the *M* component of the measured velocity expressed in the averaged magnetopause coordinates LMN. Substantial data points are distributed in blue box in figure 5, and the high-speed low-density feature can be seen in the Ni-Vm plot.~~In this event, there are few measurements distributed in the high-speed and low-density region, indicating that the high-speed and low-density feature was not seen in the V_m-N_i plot (figure 5).~~ ~~However~~Hence then, the rotations of the plasma flows, the ~~stretching~~ perturbations of the magnetic field~~ lines~~, the high-velocity and low density feature, and the distortions of the magnetopause ~~indicated~~ support the formation of rolled-up K-H vortices. It is worth noting that the first peak arrived as soon as the IMF turned northward at UT 22:22, ~~while~~ which ~~no pre-existing denser boundary layer resulting from high latitude reconnections was needed to~~can facilitate the K-H instability~~ as previously described (Hasegawa et al., 2009; Nakamura et al. 2017)~~.

Before and after the UT 22:22-22:52 interval, the magnetospheric hot ions dominated in panel 5 of figure 2, mainly in the ~~5~~3-25 keV range with an energy flux of 10^6 eV/(cm^2-s-sr-eV), and the magnetospheric hot electrons dominated in panel 6, mainly in the 0.5-25 keV range with an energy flux of over 10^7 eV/(cm^2-s-sr-eV). The typical temperatures of magnetospheric hot ions and electrons were about 4 keV and 0.3 keV, respectively. On the other hand, during the UT 22:22-22:52 interval, the repeating magnetosheath cold ions in panel 5 were primarily observed between 0.1-3 keV with an energy flux of over 10^6 eV/(cm^2-s-sr-eV), and the cold electrons in panel 6 were observed between 10-500 eV, with an energy flux of over 10^7 eV/(cm^2-s-sr-eV). The typical temperatures of magnetosheath cold ions and electrons were about 0.2 keV and 0.05 keV, respectively. Embedded in the plasmas of the two different origins, the coexisting hot and cold ions overlapped. ~~The alternating shifts of the hot and cold ions appeared more periodic at the upstream location of TH-A (panel 5 in figure 2), but more dispersed at the downstream TH-E.~~ Taking the mass ratio of protons to electrons into account, the gyro-radius of the electrons is only 1/42 of protons with the same energy and the same magnetic field, estimated to be approximately 2 km. We understand the ion ~~mixture/~~transport as the coexistence of magnetosheath and magnetospheric ions in the observations, characterized by the ~~observed~~ substantial ~~magnetosheath~~ cold ions in the steady background of the ~~magnetospheric~~ hot plasma~~ (and vice versa)~~. For the proton's gyro-radius of approximately 80-100 km at the magnetopause, the coexistence of the hot and cold ions in the spectrum is not sufficient to diagnose the mixture of the two components. Thus, we used the observed hot electrons as an additional indicator of the magnetosphere region because of their relatively smaller gyro-radius. Hence, the criteria to identify the mixture/transport are described such that the cold ions of 0.1-3 keV can be observed with an energy flux over 10^5 eV /(cm^2-s-sr-eV) in the hot ions background, with an energy flux over 10^6 eV /(cm^2-s-sr-eV), as well as a substantial enhancement in the energy flux of the hot electrons of 0.5-5 keV. Based on such criteria, the ion mixture/transport intervals were diagnosed from both TH-A and TH-E, marked by the green bars at the bottom of panel 6 and the black bars at the bottom of panel 10 in figure 2. The transport ~~regions in~~regions in the TH-A observations (green bars) –were distributed at the edges of the vortices and appeared to be more periodic, while those in the TH-E observations (black bars) were more dispersive.

The coexistence of hot and cold ions is one direct feature of the solar wind transport into

带格式的：字体：倾斜

带格式的：缩进：首行缩进： 1 字符

the magnetosphere, as clearly displayed in Geotail observations by Fujimoto et. al. (1998) and in Cluster observations by Hasegawa et. al. (2004). In this event, the coexistence of hot and cold ions was firstly noted near the periodically oscillating magnetopause. Furthermore, we used the enhancement of hot electron flux as an indicator of the magnetosphere, and set up the more critical criteria to diagnose the coexistence, and hence to display the transport regions, as marked by the green bars at the bottom of panel 6 and black bars at the bottom of panel 10 in figure 2. The evidence of the plasma transport is clearly shown in this event. By comparing the green bars and the black bars, it can be found that the transport regions in TH-A observations appears more periodic but those in TH-E observations more dispersed. The difference between the features of transport regions at upstream TH-A and downstream TH-E implies the plasma transport significantly occurred and evolved during the tailward propagation, along with the collapse of the vortices, leading to a kind of turbulence state, as illustrated in previous simulations (Nakamura et al., 2004; Matsumoto & Hoshino, 2004).

TH-A observed very clearly periodic motions of magnetopause during the 34 minutes except UT 22:46-22:50, TH-E observed relatively much more dispersed spectrum during the interval but 5 clear oscillations appeared again during UT 22:40-22:48. However, it seems true that, on the whole, the spectrum observed at TH-E is much more turbulent than the periodic spectrum at TH-A. Such an evolution implies the collapse of the vortices and the evolution leading to turbulence state. In previous simulations (Nakamura et al., 2004; Matsumoto & Hoshino, 2004), the vortices collapse and cause transport of the solar wind into magnetosphere, after that, new vortices may be generated at the recovered magnetopause. The 5 oscillations during UT 22:40-22:48 at downstream TH-E can by explained as newly formed vortices.~~This feature was also found in the alternating encounters of the magnetosheath and magnetosphere ions in the spectra (panels 5 & 9 in figure 2). This outcome means that substantial solar wind transport into the magnetosphere occurred during the tailward propagation from TH-A to TH-E~~. As mentioned above, the first K-H wave, as well as the ~~mixture~~ transport regions arrived at the upstream TH-A as soon as the IMF abruptly turned northward. The K-H vortices were evidently activated as a response to the abrupt northward turning of the IMF, ~~and no pre-existing denser boundary layer resulting from the high latitude reconnections was needed~~ which was the direct change to facilitate the K-H instability immediately.

Previously, both electron and ion distributions were used to diagnose the region of observation (Chen et al., 1993). While diagnosing the ~~mixture/~~transport regions in this event, the typical plasma features in different regions were selected for comparisons (figure 6), as illustrated by the energy flux distributions of both ions (blue line) and electrons (red line). In panels 1, both the ion and electron fluxes show single-peak at the low energy, indicating the components of cold and dense magnetosheath plasma. In panel 2, the ion flux shows a double-peak, which means the coexistence of the magnetosheath cold ions and magnetospheric hot ions. The relatively smaller peak/enhancement in the electron flux show that the magnetospheric hot electrons are detected, but the cold electrons dominate, implying the spacecraft is located in magnetosheath but very close to the magnetospause, a ~~mixture~~ coexistence region. In panel 3, both the ion and electron fluxes show double-peak. The double-peak of the ion flux indicates co~~-~~existence of the magnetosheath cold ions and magnetospheric hot ions. For the electron flux, the peak at the high energy indicates that more magnetospheric hot electrons are detected, implying that the spacecraft is located in magnetosphere, another example of ~~mixture~~ coexistence region. In panel 4, both ion and electron fluxes show single-peak at the high energy, indicating the components of hot and tenuous magnetospheric plasma. It should be noted that the ion flux plots (blue lines in each panel) should be lower in the tail, but show no such decrease tails in part because the data were absent at the high energy channels. The typical regions shown correspond to the magnetosheah, the energetic particle streaming layer, the LLBL, and the magnetosphere (Sibeck, 1991).

4 Summary

We analyzed observations from TH-A and TH-E that periodically encountered the LLBL; the K-H vortices were identified by the rotation features in the bulk velocity, magnetic field deviations ~~indicating the field line stretching~~, the high-speed low-density features and the distortions of the magnetopause deduced by MVA, which indicate the generation of K-H vortices~~, without the high-speed low-density features~~. The K-H vortices started as soon as the IMF turned northward abruptly, which is ~~without any pre-existing denser boundary layer formed by high-latitude reconnections~~ the direct change to facilitate the instability immediately. By considering the enhancement of the hot electrons as an indicator of the magnetosphere region, the ion ~~mixture/~~transport regions were shown that significant plasma transport can occur during the tailward propagation from TH-A to TH-E. Typical plasma features were observed in different regions. These new observations characterized by the direct response to the northward turning of the IMF, the ~~unambiguous~~ clear evidence of plasma transport involving both ion and electron fluxes, can complement existing observations and ~~help further~~enhance our understanding of the plasma transport processes in K-H vortices.

Data Availability

The data for this paper are available at the Coordinated Data Analysis Web of NASA's Goddard Flight Center (http://cdaweb.gsfc.nasa.gov/istp_public/).

Authors Contribution

G. Q. Y. designed the idea and carried out the investigations, prepared the manuscript with contributions from all co-authors. G. K. P, C. L. C, and T. C. offered the valuable scientific discussions and helped to improve the manuscript. J. P. M. ensured the data and gave valuable suggestions. R. Y. prepared some of the figures.

Competing Interests

The Authors declare that they have no conflict of interest.

Acknowledgements

This work was supported by the Strategic Pioneer Program on Space Science, Chinese Academy of Sciences, Grant No. XDA15052500, XDA15350201, and XDA17010301, and by the National Natural Science Foundation of China, Grant No. 41574161, 41731070, 41574159 and 41004074. ~~The data for this paper are available at the Coordinated Data Analysis Web of NASA's Goddard Flight Center (http://cdaweb.gsfc.nasa.gov/istp_public/).~~ The authors are grateful to NASA's Goddard Flight Center and the associated instrument teams for supplying the data. The Authors thank Professor Chi Wang and Professor Lei Dai for valuable scientific discussions. The authors also express their thanks for the support from the Specialized Research Fund for State Key

带格式的：字体：加粗

带格式的：缩进：首行缩进： 1 字符

带格式的：字体：小四，加粗

带格式的：字体：加粗

带格式的：缩进：首行缩进： 2 字符

带格式的：字体：小四，加粗

带格式的：缩进：首行缩进： 1 字符

Laboratories and the CAS-NSSC-135 project．Part of the work was done during G. Q. Yan's visit at UC Berkeley, who cordially appreciates the assistance from Professor Forrest S. Mozer.

References

Adamson, E., Nykyri, K., and Otto, A.: The Kevin-Helmholtz instability under Parker-Spiral interplanetary Magnetic Field conditions at the magnetospheric flanks, Adv. Space Res., 58, 218-230, 2016.

Angelopoulos, V.: The THEMIS mission, Space Sci. Rev., 141, 5–34, doi:10.1007/s11214-008-9336-1, 2008.

Angelopoulos, V., The ARTEMIS mission, Space Sci. Rev., 165, 3–25, doi:10.1007/s11214-010-9687-2, 2011.

Auster, U., Glassmeier, K. H., Magnes, W., Aydogar, O., Baumjohann, W., Constaninescu, D., Fischer, D., Fornicon, K. H., Georgescu, E., Harvey, P., Hillenmaier, O., Kroth, R., Ludlam, M., Narita, Y., Nakamura, R., Okrafca, K., Plaschke, F., Richter, I., Schwartzl, H., Stoll, B., Vanavanoglou, A., Wiedemann, M.: The THEMIS fluxgate magnetometer, Space Sci. Rev., 141, 235–264, doi:10.1007/s11214-008-9365-9, 2008.

Chaston, C. C., Wilber, M., Mozer, F. S., Fujimoto, M., Goldstein, M. L., Acuna, M., Rème, H., and Fazakerley, A.: Mode conversion and anomalous transport in Kelvin-Helmholtz vortices and kinetic Alfven waves at the Earth's magnetopause, Phys. Rev. Lett., 99, 175004, Doi: 10.1103/PhysRevLett.99.175004, 2007.

Chen, Q., Otto, A., and Lee, L. C.: Tearing instability, Kelvin-Helmholtz instability, and magnetic reconnection, J. Geophys. Res., 102(A1), 151-161, 1997.

Chen, S. H., and Kivelson, M. G.: On nonsinusoidal waves at the magnetopause, Geophys. Res. Lett., 20, 2699-2702, 1993.

Chen, S.-H., Kivelson, M. G., Gosling, J. T., Walker, R. J., and Lazarus, A. J.: Anomalous aspects of magnetosheath flow and of the shape and oscillations of the magnetopause during an interval of strongly northward interplanetary magnetic field, J. Geophys., 98, 5727-5742, 1993.

Dai, L.: Collisionless Magnetic Reconnection via Alfven Eigenmodes, Phys. Rev. Lett., 102, 245003, doi:https://doi.org/10.1103/PhysRevLett.102.245003, 2009.

Dai, L., Wang, C., Zhang, Y., Lavraud, B., Burch, J., Pollock, C., and Torbert, R. B.: Kinetic Alfvén wave explanation of the Hall fields in magnetic reconnection, Geophys. Res. Lett., 44, 634–640, doi:10.1002/2016GL071044, 2017.

Dai, L.: Structures of Hall Fields in Asymmetric Magnetic Reconnections, J. Geophys. Res. Space Physics, 123(9), 7332-7341, doi: https://doi.org/10.1029/2018JA025251, 2009.

Dungey, J. W.: Interplanetary magnetic field and auroral zones, Phys. Rev. Lett. 6(2), 47-48, 1961.

Farrugia, C. J., F. T. Gratton, G. Gnavi, R. B. Torbert, L. B. Wilson, A vortical dawn flank boundary layer for near-radial IMF: Wind observations on 24 October 2001, J. Geophys. Res. Space Physics, 119, 4572-4590, doi: 10.1002/2013JA019578, 2014.

Fujimoto, M., Terasawa, T., Mukai, T., Saito, Y., Yamamoto, T., and Kokubun, S.: Plasma entry from the flanks of the near-Earth magnetotail: Geotail observations, J. Geophys.Res. 103(A3), 4391-4408, 1998.

Fujimoto M., Tonooka, T., and Mukai, T.: Vortex-like fluctuations in the magnetotail flanks and their possible roles in plasma transport in the Earth's Low-Latitude Boundary Layer, Geophys.

Monogr. Ser., vol. 133. Edited byNewell, P. T., and Onsager, T., p. 241, AGU., Washington D. C., 2003.

Grygorov, K., Němeček, Z., Šafránková, J., Přech, L., Pi, G., Shue, J.-H.: Kelvin-Helmholtz wave at the subsolar magnetopause boundary layer under radial IMF. J. Geophys., Res. Space Physics, 121, 9863-9879, doi: 10.1002/2016JA023068, 2016.

Hasegawa, A.: Plasma instabilities and Non-linear effects, Springer-Verlag, New York, 1975.

Hasegawa, H., Fujimoto, M., Phan, T.-D., Rème, H., Balogh, A., Dunlop, M. W., Hashimoto, C., and TanDokoro, R.: Transport of solar wind into Earth's magnetosphere through rolled-up Kelvin-Helmholtz vortices. Nature, 430, 755-758, doi:10.1038/nature02799, 2004.

Hasegawa, H., Fujimoto, M., Takagi, K., Saito, Y., Mukai, T., and Rème, H.: Single-spacecraft detection of rolled-up Kelvin-Helmholtz vortices at the flank magnetopause. J. Geophys. Res., 111, A09203, doi:10.1029/2006JA011728, 2006.

Hasegawa, H., Retinò, A., Vaivads, A., Khotyaintsev, Y., André, M., Nakamura, T. K. M., Teh, W. –L., Sonnerup, B. U. Ö., Schwartz, S. J., Seki, Y., Fujimoto, M., Saito, Y., Rème, H., and Canu, P.: Kelvin-Helmholtz waves at the Earth's magnetopause: Multiscale development and associated reconnection, J. Geophys. Res., 114, A12207, doi:10.1029/2009JA014042, 2009.

Hashmoto, C., and Fuijimoto, M.: Kelvin-Helmholtz instability in an unstable layer of finite thickness, Adv. Space Res., 37, 527, 2005.

Hwang, K.-J, Kuznetsova, M. M., Sahraoui, F., Goldstein, M. L., Lee, E., and Parks, G. K.: Kelvin-Helmholtz waves under southward interplanetary magnetic field, J. Geophys. Res., 116, A08210, doi:10.1029/2011JA016596, 2011.

Hwang, K.-J., Goldstein, M. L., Kuznetsova, M. M., Wang, Y., Vinas, A. F., and Sibeck, D. G.: The first in situ observation of Kelvin-Helmholtz waves at high-latitude magnetopause during stongly dawnward interplanetary magnetic field conditions, J. Geophys. Res., 117, A08233, doi: 10.1029/2011JA017256, 2012.

Johnson, J. R., Wing, S., Delamere, P. A.: Kelvin Helmholtz Instability in Planetary Magnetospheres, Space Sci. Rev., 184, 1-31, doi: 10.1007.s11214-014-0085-z, 2014.

Kavosi, S. and Raeder, J.: Ubiquity of Kelvin-Helmholtz waves at Earth's magnetopause. Nat. Commun., 6:7019, doi:10.1038/ncomms8019, 2015

Kawano, H., Kokubun, S., Yamamoto, Y., Tsuruda, K., Hayakawa, H., Nakamura, M., Okada, T., Matsuoka, A., and Nishida, A.: Magnetopause characteristics during a four-hour interval of multiple crossings observed with GEOTAIL, Geophys. Res. Lett., 21, 2895-2898, 1994.

Kivelson, M. G., and Chen, S. H.: The magnetopause: Surface waves and instabilities and their possible dynamic consequences, in Physics of the Magnetopause, Geophys. Monogr. Ser., vol. 90. Edited by Song, P., Sonnerup, B. O. Ü., and Thomsen, M. F., p. 257, AGU., Washington D. C., 1995.

Li, W. Y., André, M., Khotyaintsev, Y. V., Vaivads, A., Graham, D. B., Toledo-Redondo, S., and Strangeway, R. J.: Kinetic evidence of magnetic reconnection due to Kelvin-Helmholtz waves. Geophys. Res. Lett., 43, 5635-5643, doi: 10.1002/2016GL069192, 2016.

Manuel, J. R., and Samson, J. C.: The Spatial Development of the Low-latitude Boundary Layer. J. Geophys. Res., 98(A10), 17367-17385, 1993.

Masson, A., and Nykyri, K.: Kelvin-Helmholtz Instability: Lessons Learned and Ways Forward. 214, 71-89, doi:10.1007/s11214-018-0505-6, 2018.

Matsumoto Y., and Hoshino, M.: Onset of turbulence induced by a Kelvin-Helmholtz vortex.

Geophys. Res. Lett., 31, L02807, doi: 10.1029/2003GL018195, 2004.

McFadden, J. P., Carlson, C. W., Larson, D., Ludlam, M., Abiad, R., Elliott, B., Turin, P., Marckwordt, M., and Angelopoulos, V.: The THEMIS ESA plasma instrument and in-flight calibration. Space Sci. Rev., 141, 277–302, doi:10.1007/s11214-008-9440-2, 2008.

Miura, A.: Dependence of the magnetopause Kelvin-Helmholtz instability on the orientation of the magnetosheath magnetic field. Geophys. Res. Lett., 22, 2993, 1995.

Moore, T. W., Nykyri, K., Dimmock, A. P.: Cross scale energy transport in space plasmas. Nat. Phys., 12, 1164-1169, doi: 10.1038/nphys3869, 2016.

Mozer, F. S., Hayakawa, H., Kokubun, S., Nakamura, M., Okada, T., Yamamoto, T., and Tsuruda, K.: The morningside low-latitude boundary layer as determined from electric field and magnetic field measurements on Geotail, Geophys. Res. Lett., 21, 2983, 1994.

Nakamura, T. K. M., Hayashi, D., and Fujimoto, M.: Decay of MHD-Scale Kevin-Helmholtz Vortices Mediated by Parasitic Electron Dynamics. Phys. Rev Lett., 92(14), 145001, doi: 10.1103/PhysRevLett.92.14501, 2004.

Nakamura, T. K. M., Eriksson, S., Hasegawa, H., Zenitani, S., Li, W. Y., Genestreti, K. J., Nakamura, R., and Daughton, W.: Mass and Energy Transfer across the Earth's Magnetopause Caused by Vortex-Induced Reconnection, J. Geophys. Res.: Space Physics, 122, 11505-11522, doi: 10.1002/2017JA024346, 2017.

Nykyri, K., and Otto, A.: Plasma transport at the magnetospheric boundary due to reconnection in Kelvin-Helmholtz vortices, Geophys. Res. Lett., 28, 3565-3568, 2001.

Nykyri, K., Otto, A., Lavraud, B., Mouikis, C., Kistler, L. M., Balogh, A., and Rème, H.: Cluster observations of reconnection due to the Kelvin-Helmholtz instability at the dawnside magnetosphere flank, Ann. Geophys., 24, 2619-2643, 2006.

Otto, A, and Fairfield, D. H.: Kelvin-Helmholtz instability at the magnetotail boundary: MHD simulation and comparison with Geotail observations, J. Geophys. Res., 105(A9), 21175-21190, 2000.

Sergeeve, V. A., Sormakov, D. A., Apatenkov, S. V., Baumjohann, W., Nakamura, R., Runov, A. V., Mukai, T., and Nagai, T.: Survey of large-amplitude flapping motions in the midtail current sheet, Ann. Geophys., 24, 2015-2024, 2006.

Shue, J.-H., Song, P., Russell, C. T, Steinberg, J. T., Chao, J. K., Zastenker, G., Vaisberg, O. L., Kokubun, S., Singer, H. J., Detman, T. R., and Kawano, H.: Magnetopause location under extreme solar wind conditions, J. Geophys. Res., 103, 17691-17700, 1998.

Sibeck, D. G.: Transient event in the Outer magnetosphere: boundary waves or flux transfer event? J. Geophys. Res., 97(A4), 4009-4026, 1992.

Sckopke, N., Paschmann, G., Haerendel, G., Sonnerup, B. U. Ö., Bame, S. J., Forbes, T. G., Hones Jr, E. W., andRussell, C. T.: Structure of the Low- Latitude Boundary Layer, J. Geophys. Res., 86(A4), 2099-2110, 1981.

Sonnerup, B. U. Ö., and Cahill, L. J.: Magnetopause structure and attitude from Explorer 12 observations, J. Geophys. Res., 72, 171-183, 1967.

Sonnerup, B. U. Ö., and Cahill, L. J.: Explorer 12 observations ~~O~~of the magnetopause current layer, J. Geophys. Res., 73, 1757-1770, 1968.

Song P., and Russell, C. T.: Model of the formation of the low-latitude-boundary-layer for strongly northward interplanetary magnetic field, J. Geophys. Res., 97(A2), 1411-1420, doi, 10.1029/91JA02377, 1992.

Southwood, D. J.: Magnetopause Kelvin-Helmholtz instability, in Magnetosphere Boundary Layers, edited by Battrick, B., and Mort, J., pp. 357-364, European Space Agency Scientific and Technical Publications Branch, Noordwijk, The Netherlands, 1979.

Tang, B. B., Wang, C., and Li, W. Y.: The magnetosphere under the radial interplanetary magnetic field: A numerical study, J. Geophys., Res. Space Physics, 118, 7674-7682, doi: 10.1002/2013JA019155, 2013.

Walsh, B. M., Thomas, E. G., Hwang, K. -H., Baker, J. B. H., Ruohoniemi, J. M., Bonnell, J. W.: Dense plasma and Kelvin-Helmholtz waves at Earth's dayside magnetopause, J. Geophys. Res.: Space Physics, 120, 5560-5573, doi: 10. 1002/2015JA021014, 2015.

Yan, G. Q., Shen, C., Liu, Z. X., Rème, H., Carr, C. M., and Zhang, T. L.: A Statistical Study on Correlations between Plasma Sheet and Solar Wind Based on DSP Explorations, Ann. Geophys., 23, 2961-2966, 2005.

Yan, G. Q., Mozer, F. S., Shen, C., Chen, T., Parks, G. K., Cai, C. L., McFadden, J. P.: Kelvin-Helmholtz Vortices observed by THEMIS at the duskside of the magnetopause under southward IMF. Geophys. Res. Lett., 41, 4427-4434, doi:10.1002/2014GL060589, 2014.

Figures and Captions

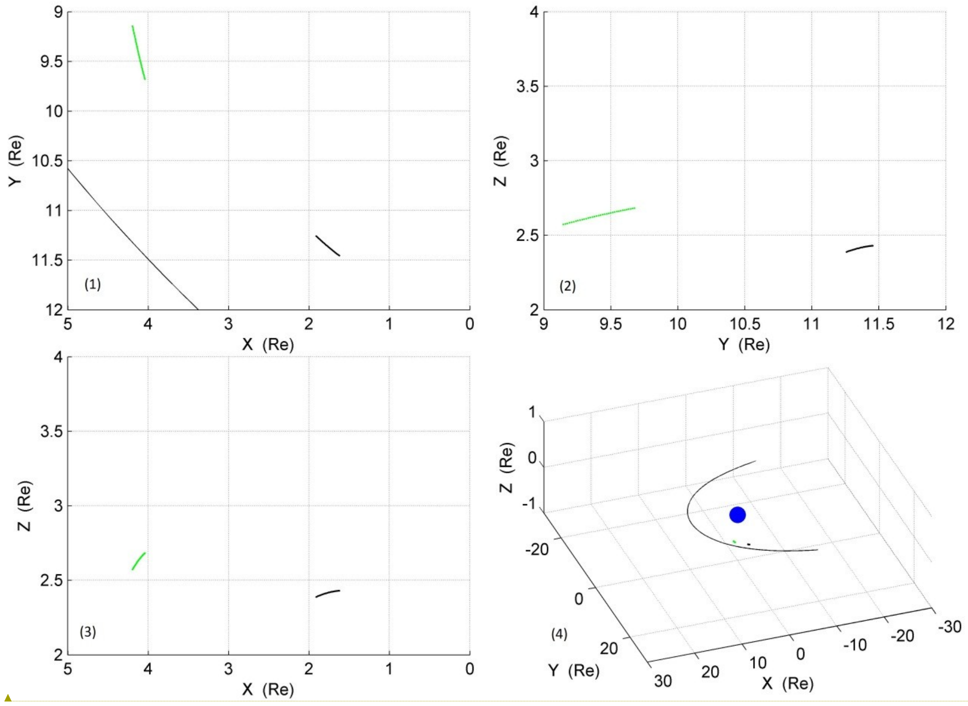

.

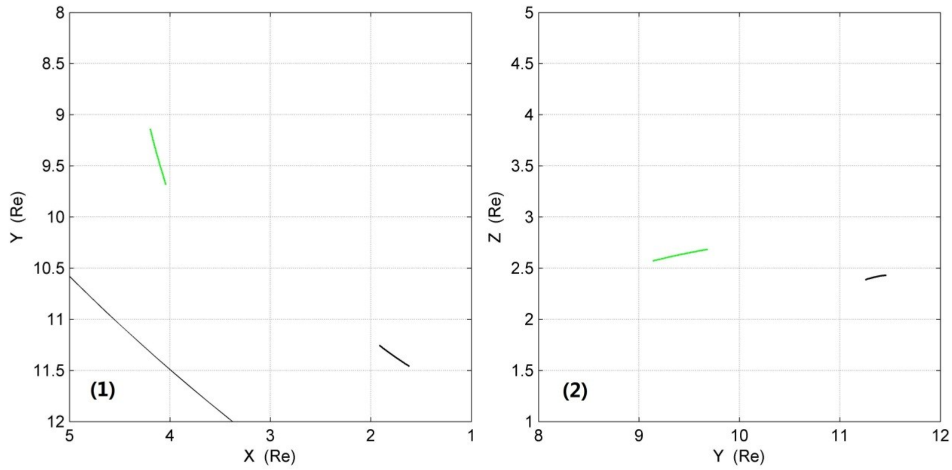

Figure 1. The orbits and positions of TH-A (green) and TH-E (black) during the interval of interest UT 22:20 ~ UT

带格式的: 字体: (默认) Times New Roman

带格式的: 字体: (默认) Times New Roman

22:54. The position data are expressed in GSM coordinates.

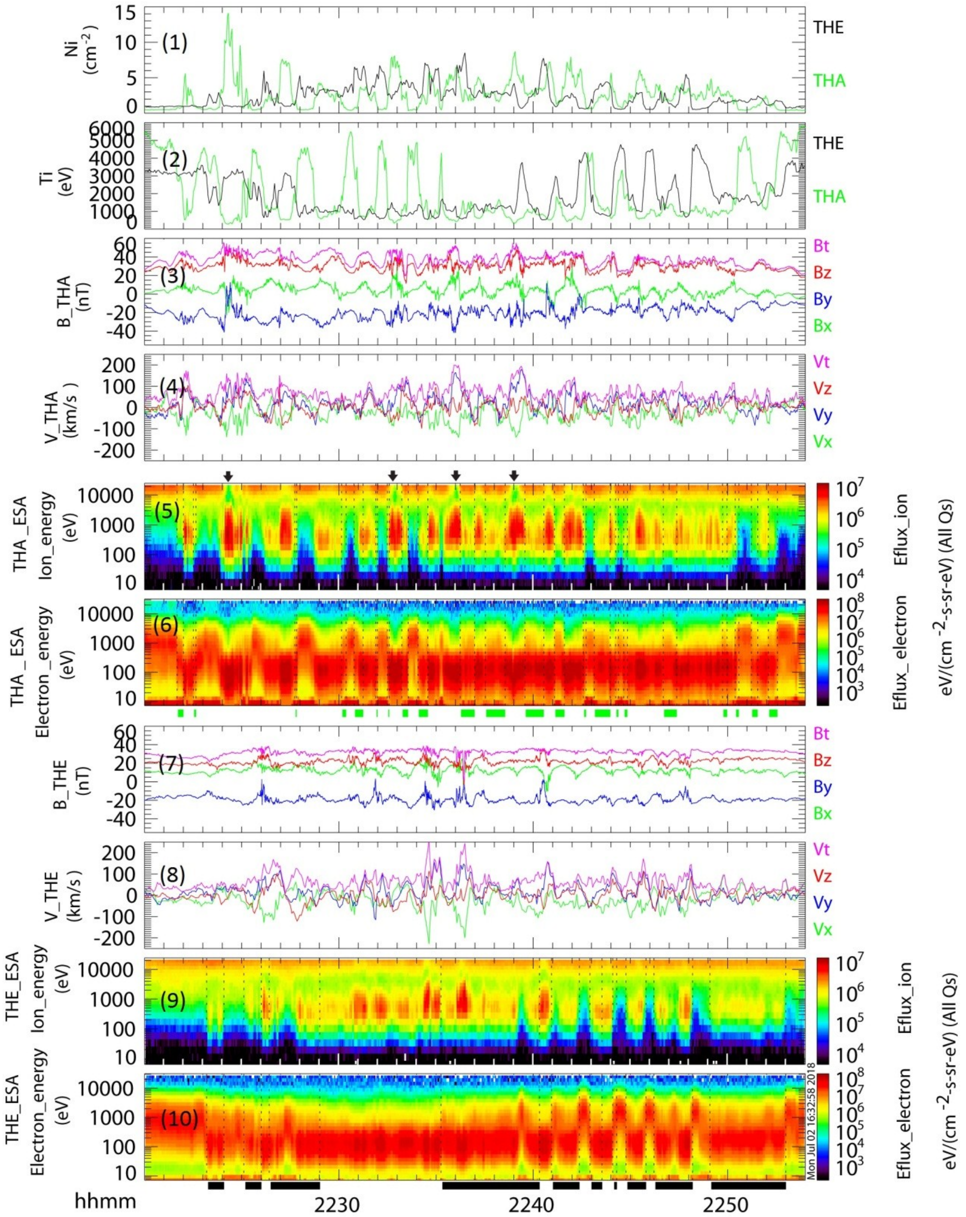

Figure 2. Fluctuations in the plasma parameters and the ion and electron energy-time spectra. Panel 1 is the ion densities from TH-A as a green line and from TH-E as a black line; panel 2 is the ion temperatures from TH-A as a green line and from TH-E as a black line; panels 3 and 4 are the magnetic field vectors and the ion bulk velocity vectors from TH-A, respectively; panels 5 and 6 are the ion and electron energy-time spectra from TH-A, respectively; panels 7 and 8 are the magnetic field vectors and the ion bulk velocity vectors from TH-E, respectively; panels 9 and 10 are the ion and electron energy-time spectra from TH-E, respectively. Vectors are all expressed in GSM coordinates. The four black arrows mark on top of panel 5 the TH-A intervals in the

magnetosheath. The green bars on the bottom of panel 5 and the black bars on the bottom of panel 9 mark the transport regions in TH-A and TH-E observations, respectively, identified based on the criteria dictated in the text.

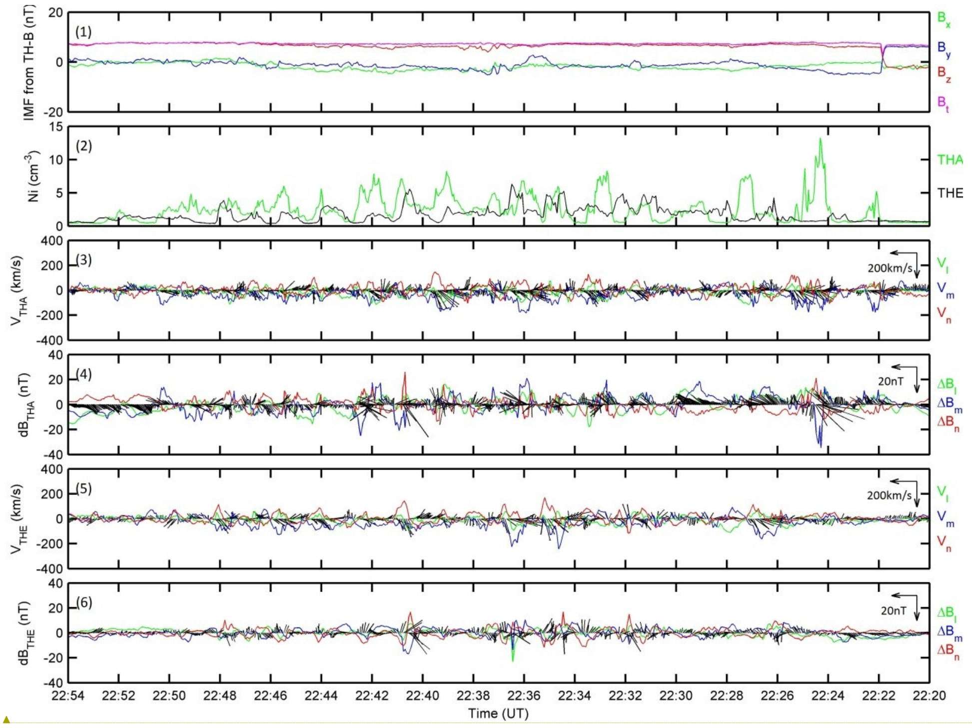

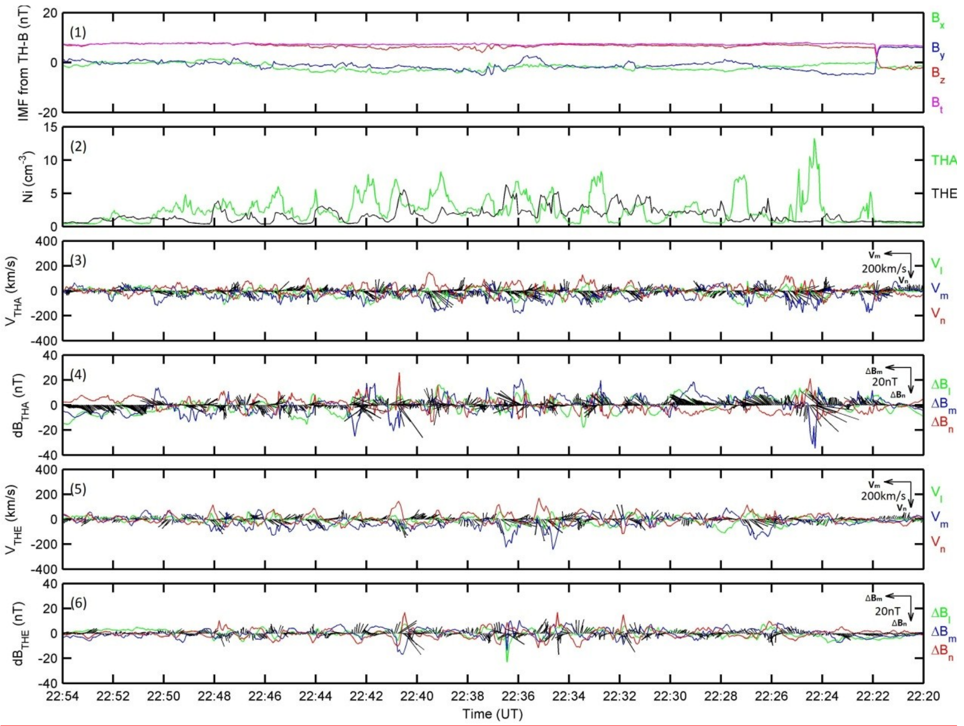

带格式的: 字体: (默认) Times New Roman

Figure 3. The observed plasma rotations and ~~stretching~~ perturbations of the magnetic field ~~lines~~ because of the formation of K-H vortices. Panel 1 is the IMF monitored by TH-B near the lunar orbit, with a time lag of 10 minutes from subsolar magnetopause to TH-B; panel 2 are the ion densities from TH-A in green and from TH-E in black; panels 3 and 5 are the ion bulk velocities from TH-A and TH-E, respectively, expressed in averaged local magnetopause coordinates LMN, deduced from the magnetopause model (Shue et al., 1998); panels 4 and 6 are the magnetic field ~~deviations~~perturbations, $\Delta\boldsymbol{B}=\boldsymbol{B}-\boldsymbol{B}_{mean}$, from TH-A and TH-E respectively, expressed in LMN. Note that the time begins from the right and passes to the left, so that the M component orients leftward and N component orients downward in the plots~~.~~

Table 1. results of MVA analysis at the four magnetosheath encounters.

Num	Time interval	L	M	N	$r_{23}=\varepsilon_2/\varepsilon_3$
		0.0637	0.4374	0.8970	
1	22:23:50-22:24:12	-0.3955	-0.8141	0.4251	4.56
		0.9162	-0.3819	0.1212	
		0.0646	-0.3877	-0.9195	
2	22:24:20-22:25:15	-0.2602	0.8830	-0.3906	5.27
		0.9634	0.2645	-0.0438	
		0.0017	0.8349	0.5504	
3	22:32:30-22:32:52	-0.6860	-0.3995	0.6081	1.82
		0.7276	-0.3786	0.5721	
		-0.0561	-0.3946	-0.9171	
4	22:32:52-22:33:14	0.3303	0.8595	-0.3900	2.25
		0.9422	-0.3248	0.0821	
		0.2636	0.1004	0.9594	
5	22:35:35-22:36:00	-0.4912	-0.8420	0.2231	3.34
		0.8302	-0.5301	-0.1726	
		-0.0102	0.3363	-0.9417	
6	22:36:07-22:36:20	0.0117	0.9417	0.3362	2.77
		0.9999	-0.0076	-0.0135	
		0.2307	0.0363	0.9724	
7	22:38:41-22:39:05	-0.4125	-0.9014	0.1315	3.42
		0.8813	-0.4314	-0.1930	
		-0.0574	-0.5073	-0.8599	
8	22:39:05-22:40:30	-0.7802	-0.5145	0.3556	1.07
		0.6229	-0.6913	0.3662	

带格式的：缩进：首行缩进： 0 字符
带格式的：字体：小五
带格式的：字体：小五
带格式表格
带格式的：字体：小五
带格式的：字体：小五
带格式的：缩进：首行缩进： 2 字符
带格式的：字体：小五
带格式的：居中，缩进：首行缩进： 0 字符
带格式的：字体：小五
带格式的：缩进：首行缩进： 3 字符
带格式的：字体：小五
带格式的：字体：小五
带格式的：字体：小五
带格式的：字体：小五
带格式的：字体：小五
带格式的：字体：小五
带格式的：字体：小五
带格式的：字体：小五
带格式的：字体：小五
带格式的：字体：小五
带格式的：字体：小五
带格式的：字体：小五

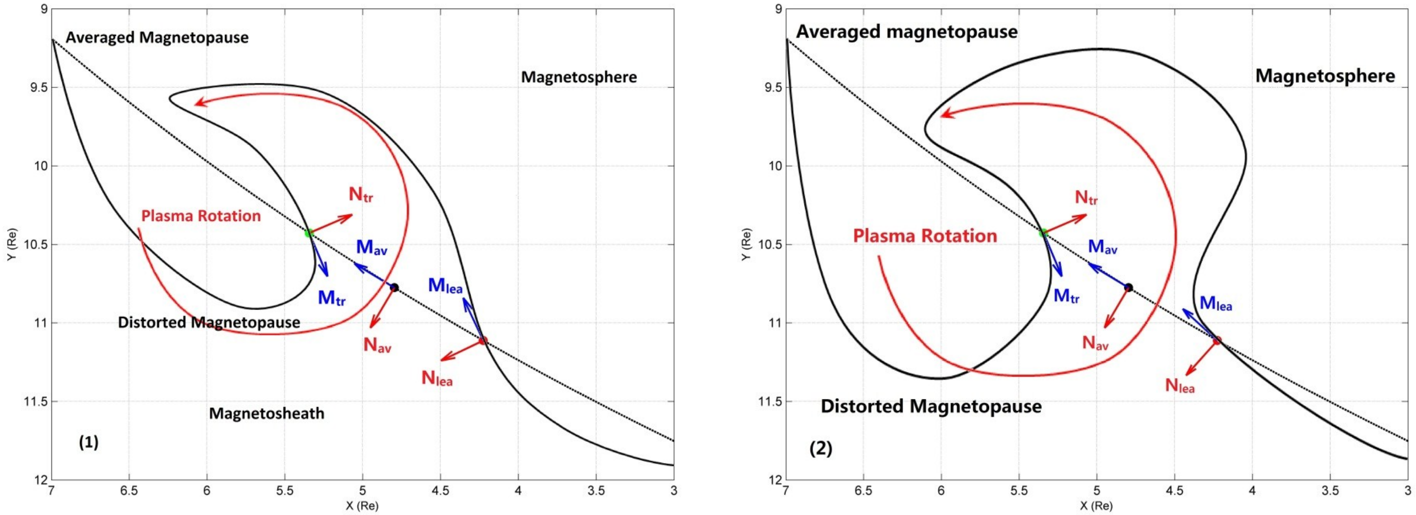

Averaged Magnetopause
Magnetosphere
Plasma Rotation
Distorted Magnetopause
Magnetosheath
(1)
Averaged magnetopause
Magnetosphere
Plasma Rotation
Distorted Magnetopause
(2)
X (Re)
Y (Re)

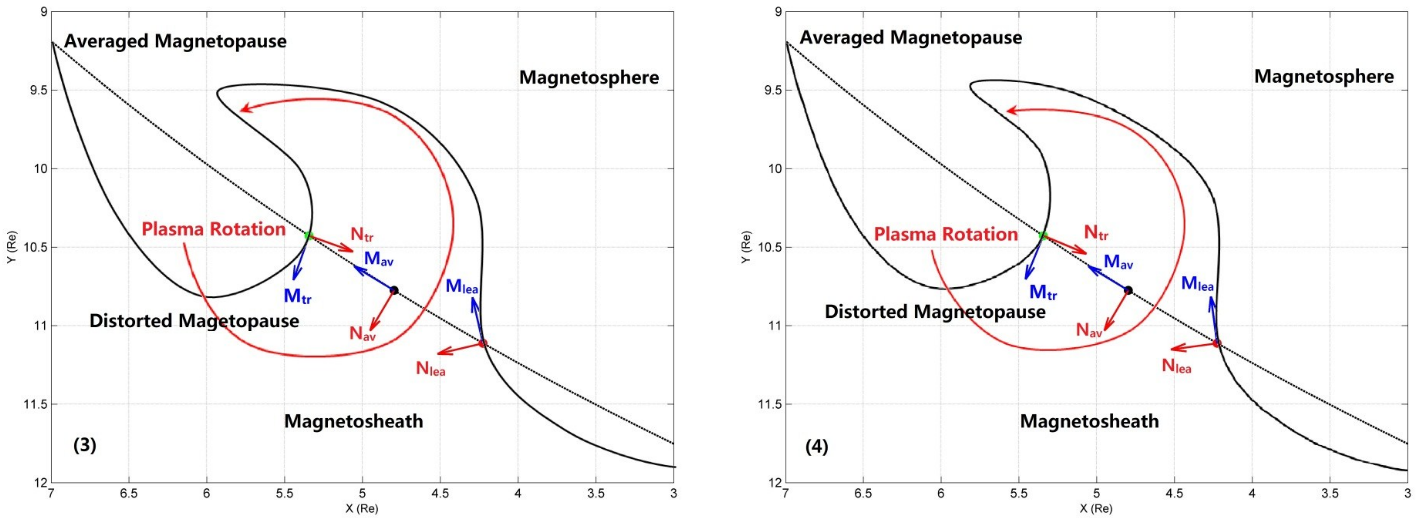

Figure 4. The magnetopause distortions formed by the K-H vortices deduced by the MVA. The average magnetopause (dashed lines), approximated to the spacecraft trajectory, was calculated from the magnetopause model (Shue et al., 1998). Traversal pair at UT 22:24 in panel 1: M_{lea}=(0.4374, -0.8141, -0.3819) and N_{lea}=(0.8970, 0.4251, 0.1212) at the outbound crossing; M_{tr}=(-0.3877, 0.8830, 0.2645) and N_{tr}=(-0.9195, -0.3906, -0.0438) at the inbound crossing. Traversal pair at UT 22:32 in panel 2: M_{lea}=(0.8349, -0.3995, -0.3786) and N_{lea}=(0.5504, 0.6081, 0.5721) at the outbound crossing; M_{tr}=(-0.3946, 0.8595, -0.3248) and N_{tr}=(-0.9171, -0.3900, 0.0821) at the inbound crossing. Traversal pair at UT 22:36 in panel 3: M_{lea}=(0.1004, -0.8420, -0.5301) and N_{lea}=(0.9594, 0.2231, -0.1726) at the outbound crossing; M_{tr}=(0.3363, 0.9417, -0.0076) and N_{tr}=(-0.9417, 0.3362, -0.0135) at the inbound crossing. Traversal pair at UT 22:39 in panel 4: M_{lea}=(0.0363, -0.9014, -0.4314) and N_{lea}=(0.9724, 0.1315, -0.1930) at the outbound crossing; M_{tr}=(-0.5073, -0.5145, -0.6913) and N_{tr}=(-0.8599, 0.3556, 0.3662) at the inbound crossing.

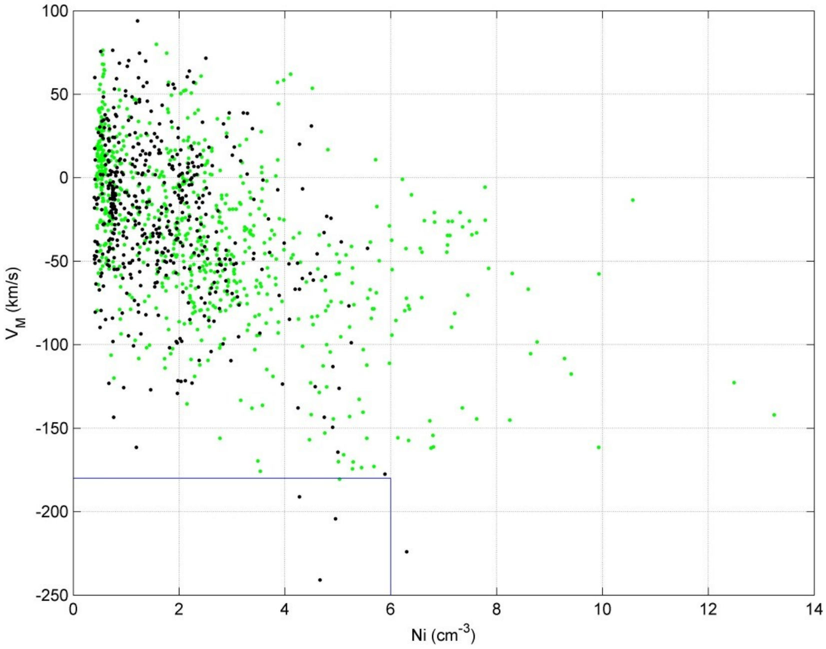

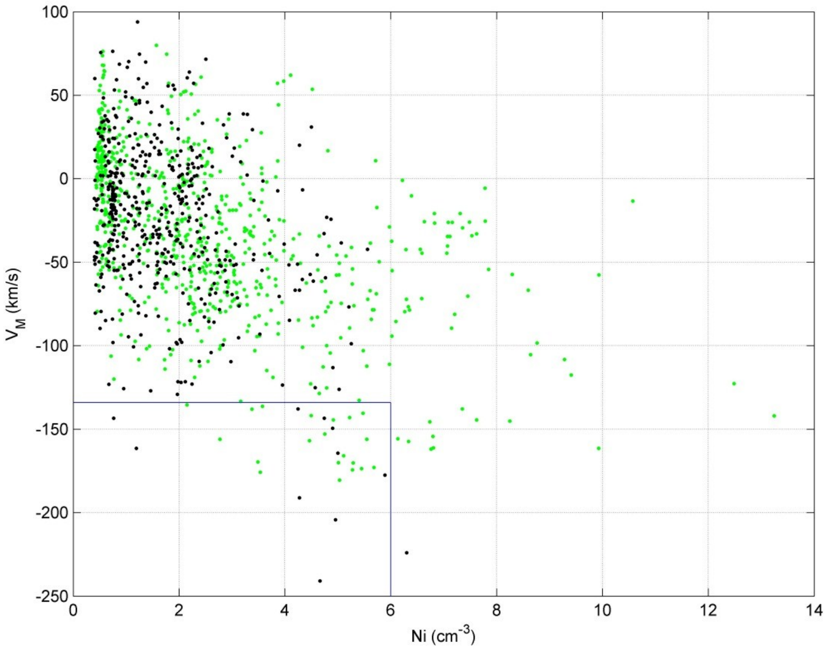

带格式的: 字体: (默认) Times New Roman, 小五

Figure 5. The observed velocity along the tailward direction versus the ion density. Green dots are from TH-A

observations and black dots from TH-E observations. The blue lines mark the high-speed and low density region possibly caused by the acceleration of the rotation.

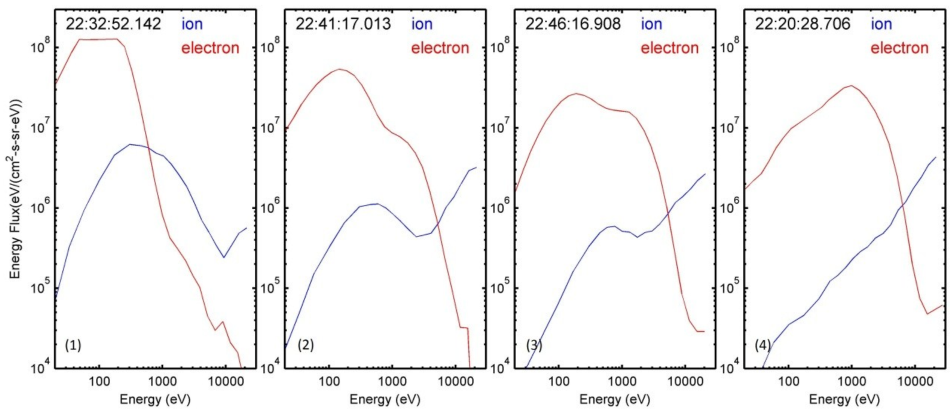

Figure 6. Typical portraits of the energy-time spectra of plasmas in different regions. Panel 1 is the magnetosheath observed by TH-A at 22:32:52.142; panel 2 is ~~mixture~~ co-existence region I observed by TH-A at 22:41:17.013; panel 3 is ~~mixture~~ co-existence region II observed by TH-E at 22:46:16.908; panel 4 is the magnetosphere observed by TH-A at 22:20:28.706.